doi:10.3772/j.issn.1006-6748.2018.01.006

Modeling approach for axial contact stiffness of ball screws①

Kong Deshun(孔德顺)* **, Wang Min②* ***, Liu Xuebin*, Gao Xiangsheng* ***
(* Beijing Key Laboratory of Advanced Manufacturing Technology, College of Mechanical Engineering and Applied Electronics Technology, Beijing University of Technology, Beijing 100124, P. R. China)
(** Institute of Standavd Metrology, Chinese Acadmy of Railway Sciences, Beijing 100081, P. R. China)
(*** Beijing Key Laboratory of Electrical Discharge Machining Technology, Beijing 100191, P. R. China)

Abstract

Axial stiffness of ball screws has great effects on accuracy of positioning, dynamic characteristic and transmission efficiency. Axial contact stiffness modeling of ball screws is the key problem in dynamic analysis of ball screws. Aiming at obtaining axial stiffness of ball screws considering microscopic fractal characteristics of contact surfaces, a new analytical method is proposed to estimate axial contact stiffness of ball screws and combine the minimum excess principle with Mandelbort (MB) fractal theory in this research. The minimum excess principle is employed to conduct normal stress analysis. And the Mandelbort fractal theory is adopted to obtain contact stiffness in ball screws. The effectiveness of the proposed method is validated by the self-designed experiment. The comparison between theoretical results and experimental results demonstrates that axial contact stiffness of ball screws could be obtained by the proposed method.

Key words: fractal theory, axial contact stiffness, ball screw, contact stress, minimum excess

0 Introduction

Ball screw is one of the most important interfaces in machine tools. The axial stiffness of ball screws has great effects on accuracy of positioning, dynamic characteristic and transmission efficiency. Many researches have been conducted on axial stiffness of ball screws. Okwudire, et al.[1,2] demonstrated theoretically and experimentally that the nut introduced a coupling between the dynamics in the axial/torsional directions and the lateral (bending) direction in ball screws. Torque-induced bending deformations were optimized to minimize the static coupling between the applied torque and lateral deformations of the screw in Ref. [3]. Uncertainty analysis of torque-induced bending deformations considering variable preload and axial stiffness was conducted in Ref. [4]. But the contact stiffness of balls was obtained by manufacturers' catalogs in the research above. Microscopic characteristics of contact surfaces is not considered in the research.

Lin, et al.[5] established a dynamic model of balls in ball screws considering frictional force and moment. Deformation in the contact region was also discussed. Wu, et al.[6] established a dynamic model of ball screws in machine tools, the axial and torsional stiffness was considered in the research. The simulation model for feed system considering the stiffness was also established. According to the equilibrium equation of forces and moments, Chen, et al.[7] established a mathematical model for stiffness of ball screws under complicated loads considering variable thread angle and deformation. Hertz theory was adopted to solve the contact status between balls and raceways. Hu, et al.[8] established an identifying approach for axial stiffness in ball screws. The axial stiffness of ball screws was identified based on experimental results. In our previous research[9], axial contact stiffness of ball screws was estimated by Hertz theory, in which the coupling relationship between the pressure of the raceway and the variation of the thread angle was considered.

Hertz theory was widely used to analyze contact status in bearings[10-12] and rolling guideways[13-15]. But for ball screws, contact region is asymmetrical because of helix angle. The greater helix angle is, the more asymmetrical the contact region is. Hertz theory can only be applied in symmetrical or axisymmetric contact faces. Relatively large error will occur when Hertz theory is applied.

Therefore, a new analytical method combining the

① Supported by the National Natural Science Foundation of China (No. 51575014, 51505012) and Natural Science Foundation of Beijing (No. KZ201410005010), China Postdoctoral Science Foundation Funded Project (No. 2016M591033) and Beijing Postdoctoral Research Foundation (No. 2015ZZ-13).

② To whom correspondence should be addressed. E-mail: wangm@bjut.edu.cn

Received on Mar. 4, 2017

minimum excess principle with Mandelbort (MB) fractal theory is proposed to estimate axial contact stiffness of ball screws in this research. Firstly, geometrical shape of contact surfaces in ball screws is analyzed, the parameter equations about screw-raceway and nut-raceway are established. 3D contact surface of raceway is simulated and meshed based on the parameter equations. Secondly, normal contact stress is solved by the minimum excess principle. Fast Fourier transform (FFT) is adopted to solve the convolution, which is used to evaluate the effect of normal stress on deformation in the normal direction. Conjugate gradient method is employed to solve the contact model. Finally, contact stiffness of the diminutive area is obtained by the MB fractal theory. The contact stiffness of contact points is calculated by integrating contact stiffness of diminutive areas. The axial stiffness of ball screws is obtained according to the connection of contact stiffness. Microscopic fractal characteristics of joints can be considered in this research. The effectiveness of the proposed method is also validated by the self-designed experiment.

1 Geometrical shape of contact surfaces

In order to facilitate the systematic study of the kinematic rules of the ball, the Cartesian coordinate and $AX_AY_AZ_A$ and $BX_BY_BZ_B$ depicted in Fig. 1 are established at contact point A between screw-raceway and ball and contact point B between nut-raceway and ball, respectively. A and B are contact points when contact just occurs. In this situation, there is no normal stress.

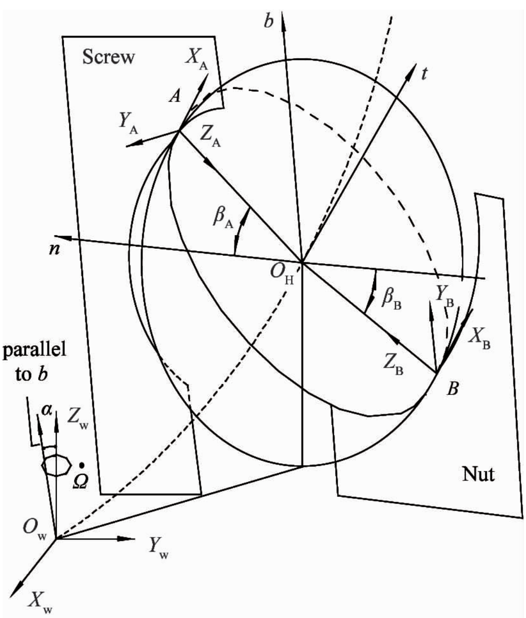

Fig. 1 Three coordinate system of ball-screw

Z_A-axis and Z_B-axis are perpendicular to the tangent plane at contact points. X_A-axis and X_B-axis are parallel to tangential direction of the center track of balls.

Geometrical shape of contact surfaces at the coordinate established at contact point $A(AX_AY_AZ_A)$ and $B(BX_BY_BZ_B)$ can be obtained by coordinate transformation.

Parameter equation of the arc in the cross section of screw-raceway at contact point A and B at Frenet-Serret coordinate system is given:

$$\boldsymbol{P}_{A(B)S}^{H} = \begin{bmatrix} 0 \\ r_{S(N)}\cos\beta_{A(B)S} - (r_{S(N)} - r_b)\cos\beta_{A(B)} \\ r_{S(N)}\sin\beta_{A(B)S} - (r_{S(N)} - r_b)\sin\beta_{A(B)} \\ 1 \end{bmatrix},$$

$$\beta_{A(B)} - \beta_{A(B)0} \leqslant \beta_{A(B)S} \leqslant \beta_{A(B)} + \beta_{A(B)0} \quad (1)$$

where r_S is the radius of arc in the cross section of screw-raceway, r_b is the radius of balls, β_A is thread angle between ball and screw-raceway, β_{AS} is central angle corresponding to the arc in the cross section of screw-raceway, β_{A0} is used to define the variation of central angle β_{AS}, r_N is the radius of arc in the cross section of nut-raceway, β_B is the thread angle between ball and nut raceway, β_{BS} is the central angle corresponding to arc in the cross section of nut-raceway, β_{B0} is used to define the variation of central angle β_{BS}.

According to the coordinate transformation, Eq. (1) is expressed as

$$\begin{aligned} \boldsymbol{P}_{AS}^{S} &= \boldsymbol{T}_{S}^{H}\boldsymbol{P}_{AS}^{H} \\ &= \begin{bmatrix} r\cos\theta - \cos\theta[r_S\cos\beta_{AS} - (r_S - r_b)\cos\beta_A] \\ r\sin\theta - \sin\theta[r_S\cos\beta_{AS} - (r_S - r_b)\cos\beta_A] \\ \cos\alpha[r_S\sin\beta_{AS} - (r_S - r_b)\sin\beta_A] \\ 1 \end{bmatrix} \\ &= \begin{bmatrix} + \sin\alpha\sin\theta[r_S\sin\beta_{AS} - (r_S - r_b)\sin\beta_A] \\ - \sin\alpha\cos\theta[r_S\sin\beta_{AS} - (r_S - r_b)\sin\beta_A] \\ + r\theta\tan\alpha \end{bmatrix} \end{aligned} \quad (2)$$

$$\begin{aligned} \boldsymbol{P}_{BS}^{S} &= \boldsymbol{T}_{S}^{H}\boldsymbol{P}_{BS}^{H} \\ &= \\ &\begin{bmatrix} r\cos\theta - \cos\theta[(r_N - r_b)\cos\beta_B - r_N\cos\beta_{BS}] \\ r\sin\theta - \sin\theta[(r_N - r_b)\cos\beta_B - r_N\cos\beta_{BS}] \\ \cos\alpha[r_N\sin\beta_{BS} + (r_N - r_b)\sin\beta_B] \\ 1 \end{bmatrix} \\ &= \begin{bmatrix} + \sin\alpha\sin\theta[(r_N - r_b)\sin\beta_B - r_N\sin\beta_{BS}] \\ - \sin\alpha\cos\theta[(r_N - r_b)\sin\beta_B - r_N\sin\beta_{BS}] \\ + r\theta\tan\alpha \end{bmatrix} \end{aligned} \quad (3)$$

where $\boldsymbol{T}_S^H$ is the coordinate transformation matrix from the coordinate system $OXYZ$, which is attached to the screw, to Frenet-Serret coordinate $O_H tnb$. $\boldsymbol{T}_S^H$ is expressed by

$$\boldsymbol{T}_{\mathrm{S}}^{\mathrm{H}} = \begin{bmatrix} -\cos\alpha\sin\theta & -\cos\theta & \sin\alpha\sin\theta & r\cos\theta \\ \cos\alpha\cos\theta & -\sin\theta & -\sin\alpha\cos\theta & r\sin\theta \\ \sin\alpha & 0 & \cos\alpha & r\theta\tan\alpha \\ 0 & 0 & 0 & 1 \end{bmatrix} \tag{4}$$

From Fig. 1, the coordinate transformation matrix from coordinate $O_{\mathrm{H}}tnb$ to $AX_{\mathrm{A}}Y_{\mathrm{A}}Z_{\mathrm{A}}$ and $BX_{\mathrm{B}}Y_{\mathrm{B}}Z_{\mathrm{B}}$ can be obtained respectively.

$$\boldsymbol{T}_{\mathrm{H}}^{\mathrm{A(B)}} = \begin{bmatrix} 1 & 0 & 0 & 0 \\ 0 & -\sin\beta_{\mathrm{A(B)}} & -\cos\beta_{\mathrm{A(B)}} & r_b\cos\beta_{\mathrm{A(B)}} \\ 0 & \cos\beta_{\mathrm{A(B)}} & -\sin\beta_{\mathrm{A(B)}} & r_{\mathrm{b}}\sin\beta_{\mathrm{A(B)}} \\ 0 & 0 & 0 & 1 \end{bmatrix} \tag{5}$$

The equation of arc in screw-raceway and nut-raceway in coordinate system $AX_{\mathrm{A}}Y_{\mathrm{A}}Z_{\mathrm{A}}$ and $BX_{\mathrm{B}}Y_{\mathrm{B}}Z_{\mathrm{B}}$ can be obtained from Eqs(2) – (5).

$$\begin{aligned} &\boldsymbol{P}_{\mathrm{A(B)S}}^{\mathrm{A(B)}} = (\boldsymbol{T}_{\mathrm{S}}^{\mathrm{H}}(\theta_{\mathrm{C}})\boldsymbol{T}_{\mathrm{H}}^{\mathrm{A(B)}})^{-1}\boldsymbol{P}_{\mathrm{A(B)S}}^{\mathrm{S}} \\ &\beta_{\mathrm{A(B)}} - \beta_{\mathrm{A(B)0}} \leqslant \beta_{\mathrm{A(B)s}} \leqslant \beta_{\mathrm{A(B)}} + \beta_{\mathrm{A(B)0}} \end{aligned} \tag{6}$$

where $\boldsymbol{T}_{\mathrm{S}}^{\mathrm{H}}(\theta_{\mathrm{C}})$ is the coordinate transformation matrix at $\theta = \theta_C$. θ_C is the central angle corresponding to the helix at A or B.

In this paper, a certain type of ball screw is studied. Geometrical shape of the raceways in the ball screw can be obtained by Eq. (6), which is depicted in Fig. 2.

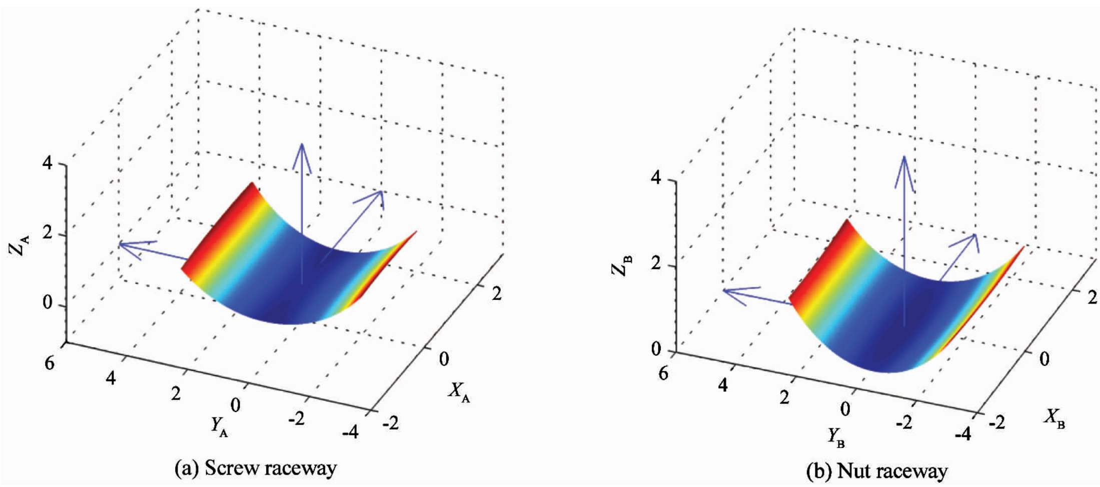

Fig. 2 Geometrical shape of the raceway

2 Normal stress analysis

Because the contact region of ball/raceway is irregular, the minimum excess principle is suitable for analyzing this problem[16,17].

The normal contact stress in every element is approximate to be constant, and the discrete form of Eq. (7) is given by

$$u_{i,j} = -\sum_{(k,l)\in I_g} K_{i-k,j-l}p_{k,l},\ (i,j)\in I_g \tag{7}$$

where $u_{i,j}$ is the normal deformation of node (i, j), $p_{k,l}$ is the normal stress subjected to the element whose center is (k, l).

$K_{i,j}$ is the influence coefficient which is defined as Ref. [18]

$$K_{i,j} = \iint_{S0} K(x_i - x', y_j - y')\mathrm{d}x'\mathrm{d}y',\ (i,j)\in I_g \tag{8}$$

where S_0 is the meshed region.

The contact problem of ball/raceway can be described as

$$\sum_{(k,l)\in Ig} K_{i-k,j-l}p_{k,l} = h_{i,j} + \delta_z,\quad (i,j)\in I_C \tag{9}$$

$$\sum_{(k,l)\in Ig} K_{i-k,j-l}p_{k,l} \geqslant h_{i,j} + \delta_z,\quad (i,j)\notin I_C \tag{10}$$

$$p_{i,j} > 0,\ (i,j)\in I_C \tag{11}$$

$$p_{i,j} = 0,\ (i,j)\notin I_C \tag{12}$$

$$d_s\sum_{(i,j)\in Ig} p_{i,j} = F_z \tag{13}$$

where δ_z is the relative rigid displacement between balls and raceways, I_C is the set of all nodes which is on the contact status, d_s is the area of element, F_z is the total normal load.

Normal contact stress $p_{i,j}$ on the contact surface can be obtained by solving Eqs (9) – (13).

Generally, the contact region is unknown before the contact problem is solved, the relative rigid displacement δ_z is also unknown, and the total normal load F_z can be calculated by preload of ball screws according to the equilibrium equation of nuts. The expression can be given by

$$F_z = \frac{F_{WS}}{n_b \cos\alpha \sin\beta} \quad (14)$$

where F_{WS} is preload of ball screws, which can be searched in manufacturers' catalogs. n_b is the number of balls on the contact status.

The contact problem is solved by conjugate gradient method to expedite convergent speed of iterative operation. In the process of iteration, deformations in the contact region is calculated from contact stress by fast Fourier transform (FFT).

In this work, 2D FFT is used to solve the elastic deformation problems between balls and raceways. Compared with other methods, FFT is more effective[19].

Detailed steps of calculation can be found in Refs[20-22].

In this study, conjugate gradient method is used to solve the contact problem, and detailed steps of calculation can be found in Ref. [23].

Normal stress on contact surface in the ball screw studied in this paper is solved by this method, which is depicted in Fig. 3. The contact region can also be predicted by Fig. 3.

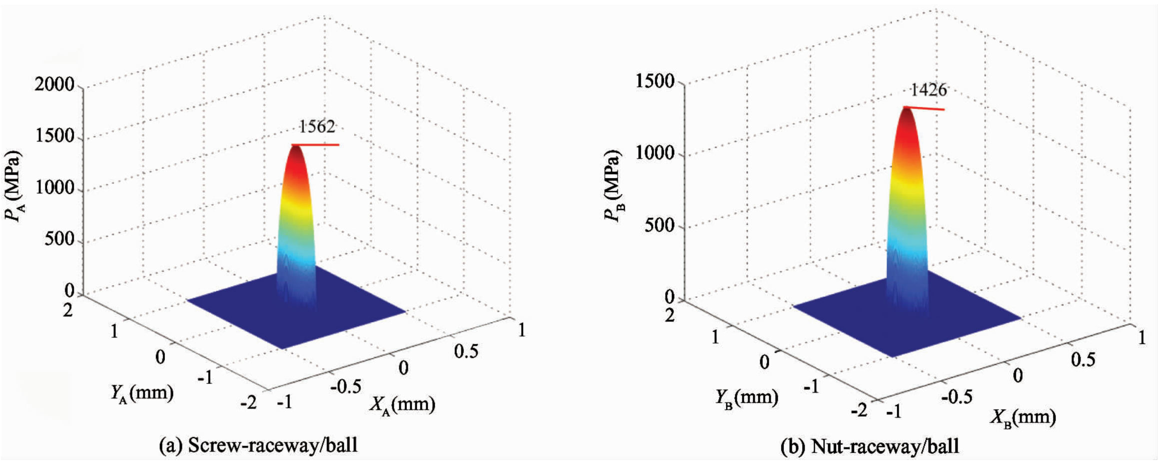

Fig. 3 Normal contact stress distribution

3 Axial contact stiffness

On the basis of contact stress obtained in Section 2, contact stiffness of every diminutive area is solved by MB fractal theory. Micro-topography of contact surfaces can be considered in MB fractal theory compared with other methods.

Contact between two contact surfaces occurs only at some discrete diminutive areas because of actual rough surfaces. The asperity on rough surfaces can be simplified to a sphere. The contact area of asperities at the critical status of elastic deformation and plastic deformation is given by

$$a_c = \frac{G^2}{(K\varphi/2)^{2(D-1)}} \quad (15)$$

where $K = \frac{H}{\sigma_y}$, $\varphi = \frac{\sigma_y}{E}$, H is the lower hardness of two contact materials, σ_y is the lower yield strength of two materials, G is scale parameter of the contact surface, D is fractal dimension of the surface profile. It describes irregular patterns of the surface profile in all the scales.

The relationship between deformation of asperities δ and its critical value δ_c can be expressed by

$$\delta_c/\delta = (a/a_c)^{D-1} \quad (1 < D < 2) \quad (16)$$

where a represents contact area of the asperity. If $a < a_c$, according to Eq. (16), $\delta_c < \delta$, plastic deformation occurs on the asperity. If $a > a_c$, $\delta_c > \delta$ can be obtained, elastic deformation occurs on the asperity.

According to the MB fractal theory, normal contact stiffness of the diminutive area is given by Ref. [24]

$$K_n = \int_{ac}^{al} 2E\sqrt{\frac{a}{\pi}} \cdot \frac{D}{2} \cdot \frac{a_l^{\frac{D}{2}}}{a^{(\frac{D}{2}+1)}} da = \frac{2EDa_l^{\frac{D}{2}}}{\sqrt{\pi}(1-D)} \cdot (a_l^{\frac{1-D}{2}} - a_c^{\frac{1-D}{2}}) \quad (17)$$

where a_l is the maximum of contact area at contact points, a_l can be solved by Eq. (18).

$$P = \frac{4\sqrt{\pi}EDG^{D-1}a_l^{\frac{D}{2}}}{3(3-2D)} \cdot (a_l^{\frac{3-2D}{2}} - a_c^{\frac{3-2D}{2}}) + \frac{k\sigma_y Da_l^{\frac{D}{2}}}{2-D} \cdot a_c^{\frac{2-D}{2}} \quad (1 < D < 2,\ D \neq 1.5) \quad (18a)$$

$$P = \sqrt{\pi} G^{0.5} E a_l^{0.75} \ln \frac{a_l}{a_c} + 3k\sigma_y a_l^{0.75} a_c^{0.25} \quad (D = 1.5) \tag{18b}$$

where P is the normal load on the diminutive area, and it equals to $p_{i,j}\Delta x \Delta y$, $\Delta x \Delta y$ is the area of the diminutive area.

Contact stiffness at contact point $A(B)$ can be obtained by

$$K_{A(B)} = \sum_{i=1}^{M} \sum_{j=1}^{N} K_{n(i,j)} \Delta x \Delta y \tag{19}$$

In this research, the mass of balls is neglected. And all the compliance is assumed to come from contact points (A and B). Therefore, the balls are modeled as massless springs having a stiffness K_{ball} aligned along the contact line between screw and nut[25]. According to the connection type of springs, the contact stiffness of balls is determined by

$$K_{ball} = \frac{K_A K_B}{K_A + K_B} \tag{20}$$

Then the axial contact stiffness is expressed as[1]

$$K_{ax} = K_{ball} n_b \cos^2\alpha \cos^2\beta \tag{21}$$

4 Validation

In order to validate the modeling approach for axial contact stiffness of ball screws proposed in this paper, self-designed experiment is implemented.

4.1 Experiment

A test scheme for axial stiffness is designed for validation. Axial stiffness is measured in a stretch test machine. The experimental setup is shown in Fig. 4. One end of the screw is fixed on the upper chuck of the machine. The nut is connected with the part which is technically designed for the experiment. The part is connected with the flange of nut via its upper end. The lower end of the part is fixed on the lower chuck of stretch test machine. Different axial tension is provided by raising or lowering the transom of the machine. Because the test result from displacement sensors on the stretch test machine is influenced by the deformations and gaps in the machine, the result differs greatly from the actual value. In this research, axial relative displacement between nut and screw is measured by an inductance micrometer. The probe of inductance micrometer is attached to the flange of nut by a magnetic base. A cross bar is fixed on the screw, and it is perpendicular to the axial direction of the inductance micrometer in a vertical plane.

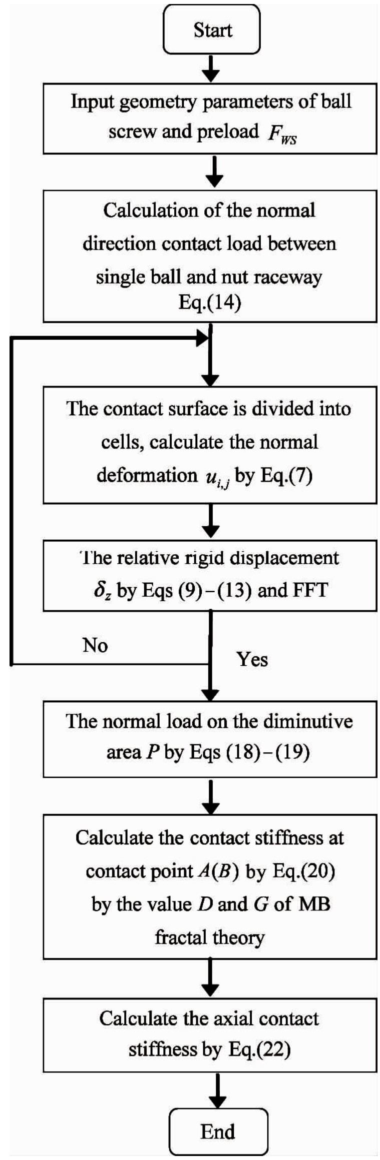

Fig. 4 Flowchart for numerical simulation of the contact stiffness by MB fractal theory

The experimental result is depicted in Fig. 5. From Fig. 5, conclusion can be drawn that the displacement is proportional to axial load approximately. The axial contact stiffness K_{ax} can be obtained by

$$K_{ax} = \frac{\Delta F}{\Delta x} \tag{22}$$

where F is the axial load depicted in x-axis, x is the relative displacement depicted in y-axis.

4.2 Analysis and comparisons

The machining technology of balls is more mature compared with that of raceways. Therefore micro-topography of ball surface is neglected. The surface of raceway is formed by grinding. The algorithm flow chart for the numerical contact stiffness simulation by MB fractal theory is shown in Fig. 4. The specifications

Fig. 5 Experimental setup

and the experimental condition of the ball screw are shown in Table 1. According to the machining form, the fractal parameters are estimated. $D = 1.566$ and $G = 0.32$nm are introduced to the fractal theory[26]. Parameters of the ball screw studied in the experiment are also introduced to the theoretical method. Axial contact stiffness of the ball screw can be drawn that its value is 2.3117×10^8 N/m. The experimental result can be approximately obtained with its value 2.8×10^8 N/m. By comparison, the result gained by the analytical method

Table 1 ball-screw parameters

Parameters	Value	Unit
(I) Geometry parameters of the ball screw		
Screw pitch cycle radius r	16	mm
Pitch L	10	mm
Contact angle β	40.2600	°
Helix angle α	5.6833	°
Screw inner radius of screw r_{CS}	16.182	mm
Nut inner radius of screw r_{CN}	15.818	mm
Radius of curvature of the screw raceway r_S	3.215	mm
Radius of curvature of the nut raceway r_N	3.215	mm
Ball's radius r_b	2.9765	mm
Preload F_{WS}	2562.8	N
Number of balls n_b	206	
density of the ball material ρ	7.8	g/cm^3
Young's modulus E	211.1	GPa
Poisson's ratio v	0.3	
(II) The experimental conditions		
Room temperature	20	℃

in this research agrees well with the experimental result is shown in Fig. 5. The error between theoretical result and experimental result is 17%, as shown in Fig. 6. The error is acceptable in engineering practice. The error is mainly generated by the stiffness contribution of thin oil film between balls and raceways to the experimental result, which causes that the experimental result is greater than the theoretical result.

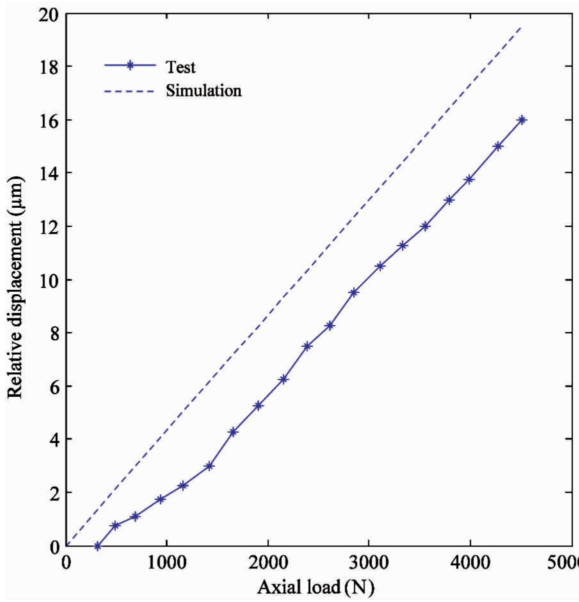

Fig. 6 Experimental results

The comparison between theoretical result and experimental result demonstrates that the analytical method combining the minimum excess principle with MB fractal theory can be implemented to estimate the axial contact stiffness of ball screws. Compared with other methods, micro-topography of contact surfaces can be considered in the analytical method proposed in this research.

5 Conclusions

It has been common practice to solve contact stiffness in ball screws by Hertz theory. But relatively large error will occur when Hertz theory is employed because of the asymmetry of contact region in the ball/raceway contact. A new analytical method combining the minimum excess principle with MB fractal theory is proposed to estimate axial contact stiffness of ball screws in this research. The minimum excess principle is employed to conduct normal stress analysis. And MB fractal theory is adopted to obtain contact stiffness in ball screws. Microscopic fractal characteristics of interfaces can be considered in this method. The effectiveness of the proposed method is validated by the self-designed experiment. The comparison between theoretical result and experimental result demonstrates that axial contact stiffness of ball screws can be obtained by the method proposed in this study.

References

[1] Okwudire C E, Altintas Y. Hybrid modeling of ball screw drives with coupled axial, torsional and lateral dynamics [J]. *Journal of Mechanical Design*, 2009, 131 (7): 071002

[2] Okwudire C E. Improved screw-nut interface model for high-performance ball screw drives[J]. *Journal of Mechanical Design*, 2011, 133(4):041009

[3] Okwudire CE. Reduction of torque-induced bending vibrations in ball screw-driven machines via optimal design of the nu[J]. *Journal of Mechanical Design*, 2012, 134 (11):3-4

[4] Gao X, Wang M, Li Q, et al. Uncertainty analysis of torque-induced bending deformations in ball screw systems [J]. *Advances in Mechanical Engineering*, 2015,7(3): 1-10

[5] Wei C C, Lin J F. Kinematic analysis of the ball screw mechanism considering variable contact deformations[J]. *Journal of Mechanical Design*, 2003,125(4):717-733

[6] Wu Q, Rui Z, Yang J. The stiffness analysis and modeling simulation of ball screw feed system[J]. *Advanced Materials Research: Manufacturing Science and Engineering*, 2010,97-101:2914-2920

[7] Chen Y, Tang W, Wang J. Influence factors on stiffness of a ball screw[J]. *Journal of Vibration and Shock*, 2013,32(11):70-74

[8] Hu F, Wu B, Shi T. Axial stiffness identification of support point for ball screw based on principle of initial parameter method[J]. *Transactions of the Chinese Society of Agricultural Machinery*, 2012,43(11):256-260

[9] Hu J Z, Wang M, Gao X, Zan T. Axial contact stiffness analysis of position preloaded ball screw mechanism[J]. *Journal of Mechanical Engineering*, 2014,50(7):60-69

[10] Guo K, Yuan S, Zhang Y, et al. Study on the calculation method of ball bearing mechanical characteristics considering elastohydrodynamic lubrication with spinning[J]. *Journal of Mechanical Engineering*, 2013,49(15):62-67

[11] Yao T, Wang L, Chi Y, et al. Multibody contact dynamics research on ball bearing[J]. *Journal of Aerospace Power*, 2013,28(7):1624-1636

[12] Guo B, Duan Z, Zheng J, et al. Double-point pitting corrosion fault diagnosis for rolling bearings of a vibrating machine[J]. *Journal of Vibration and Shock*, 2013,32 (7):58-63

[13] Jiang S, Zhu S. Dynamic characteristic parameters of linear guideway joint with ball screw[J]. *Journal of Mechanical Engineering*, 2010,46(1):92-99

[14] Liu Y, Huang Y. Theoretical analysis and experimental study on static characteristics of the cylindrical-spherical joint surfaces of linear ball guide on machine tool[J]. *Journal of Mechanical Engineering*, 2013,49(21):25-30

[15] Sun W, Kong X, Wang B, et al. Contact modeling and analytical solution of contact stiffness by Hertz theory for the linear rolling guide system[J]. *Engineering Mechanics*, 2013,30(7):230-234

[16] Jin X, Xue B, Shen Z. Principle of complementary virtual work for general contact problems and its application in research of wheel/rail contact[J]. *Journal of the China Railway Society*, 1996,18(5):30-36

[17] Polonsky I A, Keer L M. A numerical method for solving rough contact problems based on multi-level multi-summation and conjugate gradient techniques[J]. *Wear*, 1999, 231(2):206-219

[18] Johnson K L. Contact Mechanics[M]. Cambridge: Cambridge University Press,198519(2):109-110

[19] Liu S B, Wang Q. Study contact stress fields caused by surface tractions with a discrete convolution and fast Fourier transform algorithm[J]. *ASME Journal of Tribology*, 2002,124(1):36-45

[20] Wang W Z, Hu Y Z, Wang H. Numerical solution of dry contact problem based on fast Fourier transform and conjugate gradient method[J]. *Chinese Journal of Mechanical Engineering*, 2006,42(7):14-18

[21] Tian X, Bhushan B. A numerical three-dimensional model for the contact of rough surfaces by variational principle [J]. *ASME Journal of Tribology*, 1996,118(1):33-42

[22] Stanley H M, Kato T. An FFT-based method for rough surface contact[J]. *ASME Journal of Tribology*, 1997, 119(3):481-485

[23] Nocedal J, Wright S. Numerical Optimization[M]. Beijing: Science Press, 2006

[24] Zhang X, Huang Y, Han Y. Fractal model of the normal contact stiffness of machine joint surfaces based on the fractal contact theory[J]. *China Mechanical Engineering*, 2000,11(7): 727-729

[25] Zaeh M F, Oertli T, Milberg J. Finite element modeling of ball screw feed drive systems[J]. *CIRP Ann*, 2004,53 (1):289-294

[26] Ge S, Zhu H. Fractal Theory in Tribology[M]. Beijing: China Machine Press, 2005

Kong Deshun, born in 1980. He received his Ph. D. degrees in College of Mechanical Engineering and Applied Electronics Technology of Beijing University of Technology in 2017. He also received his B. S. degree in 2005 from Hebei Polytechnic University and M. S. degree from Shijiazhuang Railway Institute in 2009. His research interests include the design and calculation for key parts of CNC machine tools, analysis and control of vibration and noise of NC machine tools.